Performance Optimization in Germanium-Based Silicon Photonic Devices Using CMOS-Compatible Stressors

Andy Eu-Jin Lim, Liang Ding, Tsung-Yang Liow, Ning Duan, Mingbin Yu, and Guo-Qiang Lo

***Abstract*—Germanium (Ge)-based photonic devices are key components for silicon photonics integrated circuits. In this work, strain engineering is employed in these devices for performance optimization. Photoluminescence (PL) emission enhancement was observed for Ge epitaxial films with capping layers using standard CMOS materials. This was attributed to strain, as well as an increase in dopant density in the Ge films. The PL emission peak can either be red- or blue- shifted depending on the type of the capping layer stress. For optical detection, lateral and top stressors were incorporated in Ge photodetectors to achieve red-shifted responsivity roll-off till 1620 nm. These techniques demonstrate how light emission and detection can be optimized in Ge for optical communication applications.**

***Index Terms*—Germanium, light source, photodetector, silicon photonics, Stressor.**

I. Introduction

Intensive efforts have been devoted in Silicon (Si) -compatible photonics during the last two decades, especially in the field of active devices with remarkable progress in the last couple of years. Active building blocks have been fabricated with impressive performances on Si optical modulators and Germanium (Ge) photodetectors, and some of them have shown integration with standard complementary metal-oxide-semiconductor (CMOS) circuits or other optical components [1]-[3]. Ge has been investigated widely for active photonics devices, particularly for light detection at optical communication wavelengths (~1.3 – 1.55 μm). High performance Ge photodetectors have been realized due to its favorable absorption coefficient at these wavelengths. For dense wavelength division multiplexing (DWDM) applications in optical communications, ideally the Ge photodetectors must work in both *C* and *L* band wavelength range (1550 – 1620 nm). However, absorption roll-off is observed at wavelengths larger than 1550 nm, causing a drop in the photodetector responsivity at the *L* band. At the other end of a silicon photonics circuit, a monolithic light source is much sought after. With a direct bandgap of ~0.8 eV, light emission from Ge is in the 1.55 μm wavelength range. However, light emission efficiency is reduced due to its smaller indirect bandgap (0.66 eV). Nevertheless, photoluminescence (PL) and electroluminescence (EL) by Ge has been experimentally shown [4-6]. Still, the emission efficiency has to be improved to make it a feasible on-chip light source. A viable approach to optimize these Ge-based photonic devices is through strain engineering. The photodetector absorption edge can be shifted towards higher wavelengths through tensile strain [6]. In addition, in-plane tensile strain is able to enhance direct gap emission in Ge [7]. In this work, strain engineering on epitaxial Ge films was explored to optimize performance for photodetection and light emission applications. Standard CMOS materials such as silicon dioxide (SiO_2), silicon nitride (SiN), and amorphous silicon (a-Si) were investigated as possible stressor materials.

Manuscript received June 29, 2012; revised August 31, 2012.

The authors are with the Institute of Microelectronics, A*STAR (Agency for Science, Technology and Research), 11 Science Park Road, Science Park II, Singapore 117685 (e-mail: limej@ime.a-star.edu.sg).

II. Experiment

For light source experiments, PL measurements were conducted on blanket Ge films to determine the emission efficiency. The substrates used were 8-inch p-type Si (100) wafers. Epitaxial Ge growth of 200 nm was performed by ultra high vacuum chemical vapor deposition (UHVCVD). The Ge process consisted of a SiGe buffer layer, and a low temperature Ge seed at ~370 °C, followed by a higher temperature Ge growth at 550 °C. Double energy Phosphorus (P) implantations of 80 keV and 30 keV were carried out with a dose of 1×10^{15} cm^{-2} per implant energy to introduce n-type dopants in the Ge epi-film. Implantations at two different energies were employed to induce relatively uniform distribution of P in the Ge film. Before the dopant activation annealing, some of the samples are deposited with SiO_2, SiN, and a-Si capping films. The stresses of the blanket films were measured (See Table I). Post-implantation anneal was carried out in N_2 ambient at temperatures of 500 – 800 °C for durations of 30 – 900 s to activate dopants and recover the lattice damage caused by implantation. The PL measurements were carried out at room temperature using a Renishaw micro-PL system. The excitation source is a diode laser emitting at 785 nm with incident power of 1 mW. The light emission spectra were collected from wavelength of 1200 to 1600 nm by a GaAs detector cooled in liquid N_2 in the vertical direction through the microscope.

For waveguided photodetector (WGPD) fabrication, 8-inch SOI (220-nm Si/3-μm buried oxide) wafers were used. *p* and *p+* ion implantation into Si substrate and activation were carried out, followed by the Si waveguide (WG) etching. The Si WG has a width of 500 nm with a nano-taper width of 180 nm at the ends. A selective Ge epitaxy process was performed as per the epitaxy process described above. A total Ge thickness of 360-nm was grown on the desired region and later etched with a mask to define the PD region. Plasma enhanced chemical vapor deposition (PECVD) SiN film was deposited, and chemical-mechanical polishing

DOI: 10.7763/IJIEE.2012.V2.221

(CMP) was performed to planarize the wafer surface until the Ge surface was exposed. A 60-nm a-Si was deposited by low pressure CVD (LPCVD) to form the top compressive stressor and top contact. After *n*+ ion implantation and annealing at 700 °C, the film transited to poly-Si. The fabrication was completed with upper cladding dielectric deposition, contact hole etching, and metallization. The metallization stack used was 250Å-TaN/1-µm-Al. The schematic of the proposed Ge WGPD and the cross section of the active *p*-Si/*i*-Ge/*n*-poly-Si diode are shown in Fig. 1(a) and (b), respectively. The WGPD has a *p-i-n* structure in which the anode is formed on SOI Si while the cathode is formed on top poly-Si. The enhanced tensile stress in the Ge WGPD is realized by a lateral SiN stressor and a top poly-Si stressor.

TABLE I: SUMMARY OF CAPPING LAYER MATERIALS USED AS EPITAXIAL GE FILM STRESSOR

Stressor Material	Stress (MPa)	Type of stress
PECVD SiO_2	21	Compressive
PECVD SiN	310	Tensile
LPCVD a-Si	360	Compressive

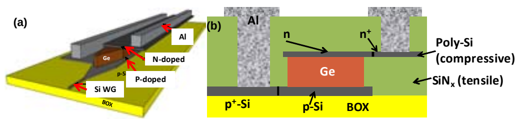

Fig. 1. (a) Schematic view and (b) cross-sectional schematic of p-i-n waveguided Ge photodetector.

III. RESULTS AND DISCUSSIONS

A. Light Source: Capping Layers for Enhanced Photoluminscence (PL) Emission

For the uncapped samples, Fig. 2(a) shows the PL spectra of the samples annealed at 500 – 800 °C for a fixed duration of 300 s, and Fig. 2(b) shows the PL spectra of the samples annealed for 30 to 900 s at a fixed temperature of 700 °C. Broad emission bands peaked at 1550 nm, consistent with the Ge direct band gap (~0.8 eV) was observed. The Ge epitaxy film had an in-situ 5 nm thick Si capping layer grown for passivation. As such, SiGe was formed on the Ge surface by Ge and Si intermixing during annealing. This was confirmed by Raman spectra (not shown) which indicated that there is Si-Ge photon mode enhanced by an increase in thermal annealing. The presence of this SiGe alloy at the surface might have led to a small blueshift of Ge direct band gap emission. The strongest PL emission is observed from the 700 °C 300 s anneal condition. This corresponds to the anneal condition which the lowest measured sheet resistance (i.e. highest electron density) was attained. Insets in Fig. 2 plot PL peak intensity with the annealing temperature or time to further support this observation. Therefore, 700 °C 300 s was used as the optimized annealing temperature for making *n*-doped Ge to emit most efficiently.

Subsequently, SiO_2, Si_3N_4, and α-Si with the thickness of 100 nm were deposited as capping layers on top of Ge before annealing at 700 °C for 300 s. The raw PL spectra for the samples with different capping layers are shown in Fig. 3(a). After correcting for the influence of the incident optical power reflectance and extraction efficiency from Ge, the PL spectra of the capped samples show much stronger intensities in Fig 3(b). Peak intensity was observed to be shifted depending on the material of capping layers [See inset Fig 3(b)]. The PL peaks of samples without a capping layer and with a SiO_2 capping layer are the same, i.e. peak intensity at 1550 nm. This indicates that the two samples have the same strain level. In contrast, the a-Si and SiN capped samples show a PL peak at 1575 nm and 1535 nm, respectively. The shifting of PL peaks is related to change of Ge direct band gap and depends on the kind of stressor layer on the Ge film. A compressively stressed a-Si film exerts a tensile stress on the Ge film and results in a blue shift in the PL peak. This effect was reported in Ref. 6 whereby the samples were mechanically strained. This work employs process-induced strain through capping layer deposition on the Ge epitaxial films. The strain on the underlying Ge film induced by the capping layers was also confirmed with Raman measurement (Fig. 4). Table II summarizes the strain in Ge film with different stressor materials. A portion of the PL enhancement was also attributed to increased dopant activation in the Ge film through reduced dopant loss during activation anneal by the capping layers. This was verified by sheet resistance measurements, and SiN capping layer had the lowest sheet resistance and exhibited the strongest PL peak intensity i.e. ~3 times of the value of the uncapped sample.

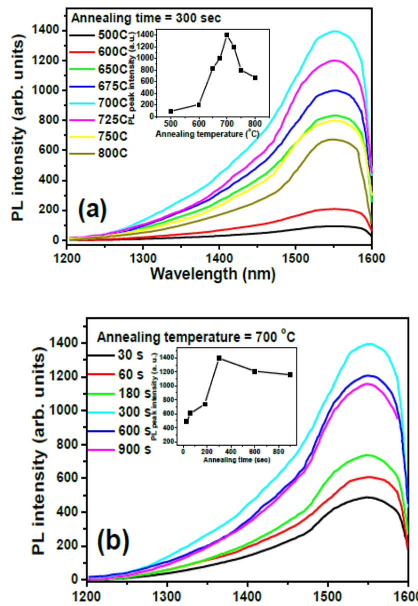

Fig. 2. (a) PL spectra for the *n*-doped Ge epi-films annealed at various temperatures for a fixed duration of 300 s. The inset shows the PL peak intensity as a function of annealing temperature. (b) PL spectra for the *n*-doped ge epi-films annealed for various durations at a fixed temperature of 700 °C. The inset shows the PL peak intensity as a function of annealing time.

TABLE II: SUMMARY OF STRAIN IN GE FILM WITH DIFFERENT CAPPING LAYERS MATERIALS.

Stressor Material	Strain in Ge (%)	Type of strain
None	0.12	Tensile
PECVD SiO_2	0.09	Tensile
PECVD SiN	0.14	Compressive
LPCVD a-Si	0.28	Tensile

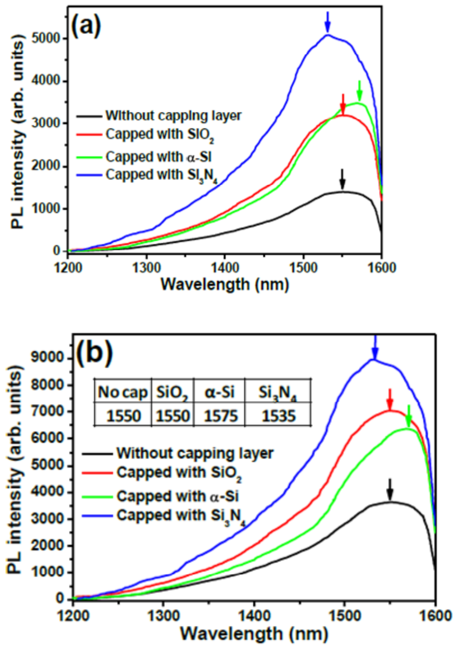

Fig. 3. (a) Directly measured PL spectra and (b) PL spectra after correction to the reflectance of pumping laser and light-out extraction efficiency of the P^+-implanted ge samples annealed with various capping layers. The inset gives the peak PL intensity for the different splits.

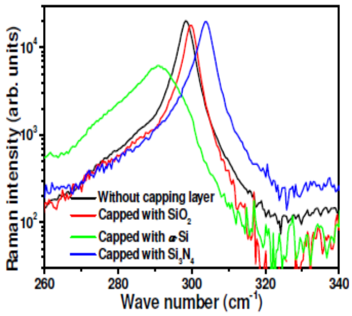

Fig. 4. High resolution raman spectra of *n*-doped ge epi film with various capping layers.

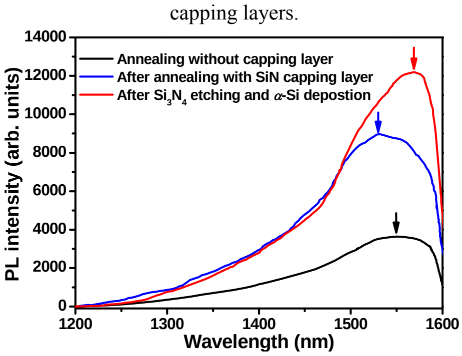

Fig. 5. PL spectra of the samples annealed without any capping layer (black), annealed with SiN capping layer (blue), and after SiN etching and a-Si deposition (red).

We observed that SiN capping is most efficient in preventing dopant loss during annealing than SiO_2 and a-Si capping layers. Moreover, it has been found that capping film not only act as diffusion block layer but also stress the Ge film to have additional strain which can impact the PL properties. In terms of additional strain in Ge, a-Si provides the tensile strain which is desired to enhance the luminescence efficiency of Ge. However, among the materials studied, no capping layers can provide both efficient blocking effect of dopant out-diffusion and additional tensile strain in Ge. Therefore, a novel process flow is proposed to optimize PL intensity. The *n*-doped Ge is first capped with SiN film and then annealed at 700 °C for 300 s. After annealing, SiN is etched away using reactive ion dry etching followed by a-Si deposition to make Ge have extra tensile strain. Fig. 5 shows that the PL emission from this novel capping layer process flow is the most efficient i.e. ~4 times of that as compared to the sample without capping layer. At the same time, the PL peak shifts to 1575 nm due to the additional tensile generated by a-Si stressor.

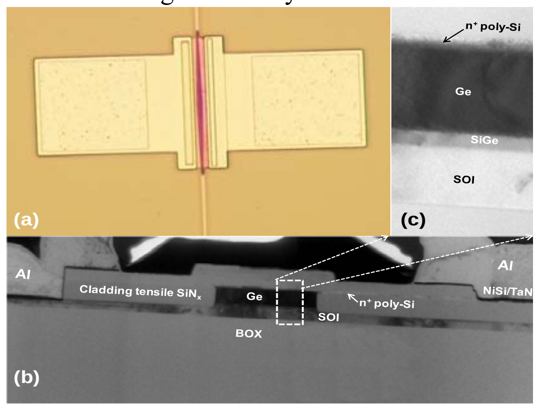

Fig. 6. (a) Top view micro-photograph of the fabricated device. (b) Cross sectional TEM images of the fabricated ge WGPD. (c) TEM image of active Ge region

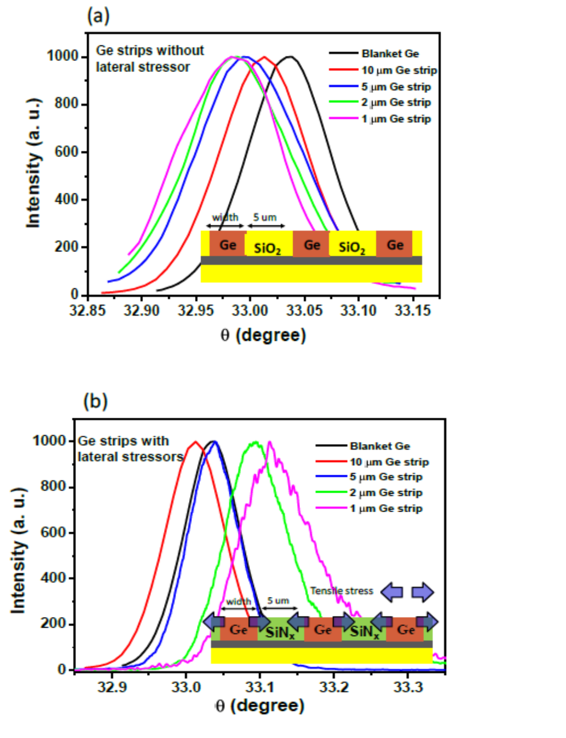

Fig. 7. High resolution XRD spectra for ge array (a) without and (b) with SiN lateral stressors. Insets show the cross-section schematics of the ge array strips.

B. Ge Photodetector: Red-shifted Responsivity Roll-off

The micro-photograph of fabricated Ge WGPD is shown in Fig. 6(a), and the cross-sectional transmission electron microscopy (TEM) images are presented in Fig. 6(b) and (c). In the fabricated device, the exact value of strain in the Ge is not measurable with conventional X-ray diffraction (XRD) method due to the small size of detector and the presence of poly-Si/SiN on top of the Ge. The strain in the lateral SiN stressors was evaluated by Ge strip arrays with constant length of 20 μm and varying width. With such structures, the Ge strain can be measured by XRD through calculating the lattice constant. Fig. 7(a) and (b) shows the XRD intensity spectra for Ge arrays without and with lateral SiN stressor. The shift in the intensity peaks as the Ge width varies show a change in strain in the Ge film. Fig. 8 shows the calculated in-plane tensile strain from XRD measurement as a function of Ge strip width for the arrays with and without lateral stressors. Without lateral stressor, the residual strain decreases with Ge width from 0.046% to 0 for 10 to 1 μm, respectively. This shows that biaxial strain in Ge film decreases as it reduces in size. As a reference, a blanket Ge film grown using the same epitaxy process described above has a tensile strain of 0.126%. On the other hand, when the Ge strips are embedded in the lateral stressors, the tensile stress in the Ge increases with decreasing width to a maximum value of 0.327% at 1 μm width. This is the effect of uniaxial tensile strain on the narrow Ge strip by the adjacent SiN stressors. For device fabrication, the Ge width was chosen to be 2 μm. It should be pointed out that the 2 μm Ge in the final device has the tensile stress larger than 0.267% (calculated in Fig. 8), because the additional stress coming from the top poly-Si stressor is not reflected.

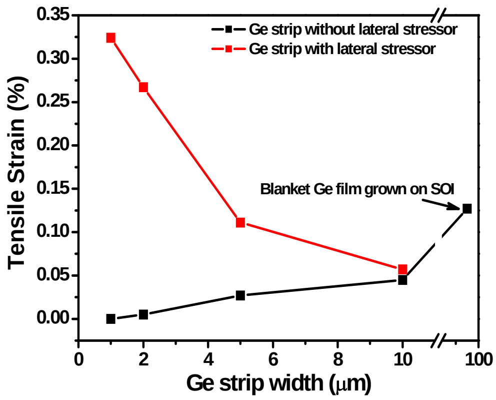

Fig. 8. In plane tensile strain in ge strip arrays for ge with and without SiN lateral stressors. The residue strain in blanket ge film grown on SOI is shown for reference.

For responsivity measurements, the optical signal was coupled into the Si waveguide (WG) using a lensed fiber. Prior to calculating the responsivity, the coupling loss between fiber and Si WG, and WG propagation loss were measured from the neighbouring passive WGs followed by the calculation of the optical power reaching Ge WGPD. Three types of devices were fabricated i.e. reference WGPD without top or lateral stressor, WGPD with top stressor, WGPD with both top and lateral stressors. The responsivity of the three types of devices was measured at a bias of -1V, and is shown in Fig. 9. It is found that the WGPD without any stressors shows a clear responsivity roll-off after 1520 nm which is due to the decreased absorption in Ge. For the WGPD with only top stressor, the responsivity decreasing rate with increasing wavelength beyond 1550 nm is much smaller than the reference device without stressor, while the WGPD with both top and lateral stressors shows no obvious roll-off even after 1620 nm for the PD with both lateral and top stressors. Due to the limitation of ASE and optical filter spectral range, the responsivity at wavelength longer than 1620 nm cannot be obtained currently. The result shows that the high responsivity can be obtained at much longer wavelength by using localized structures, which is compatible with strain technology in CMOS process.

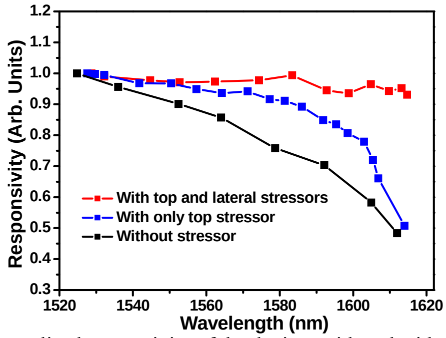

Fig. 9. Normalized responsivity of the devices with and without stressor scheme.

IV. Conclusion

We have demonstrated a systematic study on the dependences of PL from *n*-doped epitaxial Ge film. Various capping layers have been studied to enhance PL emission, and PL intensity shifts corresponds in polarity and magnitude of the strain induced in the epitaxial Ge films by these layers. In addition, the capping layers increases dopant density after annealing which also contributes to PL intensity enhancement. A novel process flow is proposed for maximizing the PL intensity by leveraging on different capping layer effects. Localized stressors were also used to demonstrate red-shift in responsivity roll-off of Ge WGPD.

References

[1] T. Y. Liow, K. W. Ang, F. Qing, J. Song, Y. Z. Xiong, M. B. Yu, G. Q. Lo, and D. L. Kwong, “Silicon modulators and germanium photodetectors on SOI: Monolithic integration, compatibility, and performance optimization,” *IEEE J. Sel. Top. Quantum Electron*, vol. 16, no. 1, pp. 307, 2010.

[2] K. W. Ang, T. Y. Liow, M. B. Yu, F. Qing, J. Song, G. Q. Lo, and D. L. Kwong, “Low thermal budget monolithic integration of evanescent-coupled Ge-on-SOI photodetector on Si CMOS platform,” *IEEE J. Sel. Top. Quantum Electron*, vol. 16, no. 1, pp. 106, 2010.

[3] A. E. J. Lim, T. Y. Liow, F. Qing, N. Duan, L. Ding, M. Yu, and G. Q. Lo, “Novel evanescent-coupled Germanium electro-absorption modulator featuring monolithic integration with germanium p-i-n photodetector,” *Opt. Express*, vol. 19, no. 6, pp. 5040, 2011.

[4] J. Liu, X. Sun, D. Pan, X. Wang, L. C. Kimerling, T. L. Koch, and J. Michel, “Tensile-strained, n-type Ge as a gain medium for monolithic laser integration on Si,” *Opt. Express*, vol. 15, pp. 11272, 2007.

[5] X. Sun, J. Liu, L. C. Kimerling, and J. Michel, “Room-temperature direct bandgap electroluminescence from Ge-on-Si light-emitting diodes,” *Opt. Letters*, vol. 34, no. 8, pp. 1198, 2009.

[6] T. H. Cheng, K. L. Peng, C. Y. Ko, C. Y. Chen, H. S. Lan, Y. R. Wu, C. W. Liu, and H. H. Tseng, “Strained enhanced photoluminescence from Ge direct transition,” *Appl. Phys Lett.*, vol. 96, pp. 211108, 2010.

[7] H.Y. Yu, D. Kim, S. Ren, M. Kobayashi, D. A. B. Miller, Y. Nishi, and K. C. Saraswat, “Effect of uniaxial-strain on Ge p-i-n photodiodes integrated on Si,” *Appl. Phys Lett.*, vol. 95, pp. 161106, 2009.